A comparison of koniocellular, magnocellular and parvocellular receptive field properties in the lateral geniculate nucleus of the owl monkey (*Aotus trivirgatus*)

Xiangmin Xu*, Jennifer M. Ichida*, John D. Allison†, Jamie D. Boyd‡, A. B. Bonds† and Vivien A. Casagrande*‡§

*Departments of *Psychology, †Electrical Engineering, ‡Cell Biology, and §Ophthalmology and Visual Sciences, Vanderbilt University, Nashville, TN 37232-2175, USA*

(Received 16 May 2000; accepted after revision 30 September 2000)

1. By analogy to previous work on lateral geniculate nucleus (LGN) magnocellular (M) and parvocellular (P) cells our goal was to construct a physiological profile of koniocellular (K) cells that might be linked to particular visual perceptual attributes.

2. Extracellular recordings were used to study LGN cells, or their axons, in silenced primary visual cortex (V1), in nine anaesthetized owl monkeys injected with a neuromuscular blocker. Receptive field centre–surround organization was examined using flashing spots. Spatial and temporal tuning and contrast responses were examined using drifting sine-wave gratings; counterphase sine-wave gratings were used to examine linearity of spatial summation.

3. Receptive fields of 133 LGN cells and 10 LGN afferent axons were analysed at eccentricities ranging from 2·8 to 31·3 deg. Thirty-four per cent of K cells and only 9% of P and 6% of M cells responded poorly to drifting gratings. K, P and M cells showed increases in centre size with eccentricity, but K cells showed more scatter. All cells, except one M cell, showed linearity in spatial summation.

4. At matched eccentricities, K cells exhibited lower spatial and intermediate temporal resolution compared with P and M cells. K contrast thresholds and gains were more similar to those of M than P cells. M cells showed lower spatial and higher temporal resolution and contrast gains than P cells.

5. K cells in different K LGN layers differed in spatial, temporal and contrast characteristics, with K3 cells having higher spatial resolution and lower temporal resolution than K1/K2 cells.

6. Taken together with previous results these findings suggest that the K cells consist of several classes, some of which could contribute to conventional aspects of spatial and temporal resolution.

In the primate lateral geniculate nucleus (LGN), three principal types of relay cells have been identified: the koniocellular (K), the parvocellular (P) and the magnocellular (M) cells. These relay cell classes can be distinguished based upon a number of criteria including laminar location, morphology, connections and neurochemistry in several primate species including bush babies, owl monkeys, marmosets and macaque monkeys (see Casagrande, 1994, 1999; Hendry & Reid, 2000 for review). K LGN cells are, on average, the smallest relay cells. They form thin layers that lie below the M and P layers, they contain the calcium-binding protein calbindin-D28k, and they send their axons to the cytochrome oxidase (CO) blobs in cortical layer III and to cortical layer I of the primary visual cortex (V1) (Lachica & Casagrande, 1992; Hendry & Yoshioka, 1994; Johnson & Casagande, 1995; Ding & Casagrande, 1997). In contrast, M and P LGN cells are large and medium in size, are located in the ventral and dorsal layers of the LGN, contain the calcium-binding protein parvalbumin and send their axons principally to the upper and lower tiers of cortical layer IVC of Brodmann (1909), respectively (Jones & Hendry, 1989; Lachica *et al.* 1992; Hendry & Yoshika, 1994; Johnson & Casagande, 1995; Ding & Casagrande, 1997; Goodchild & Martin, 1998).

The physiology of only two of these three LGN cell classes, the M and P cells, has been studied in detail across primate species (e.g. bush baby: Norton & Casagrande, 1982; Irvin *et al.* 1986, 1993; Norton *et al.* 1988; macaque monkey:

Kaplan & Shapley, 1982; Derrington & Lennie, 1984; Hubel & Livingstone, 1990; Reid & Shapley, 1992; Spear *et al.* 1994; owl monkey: Sherman *et al.* 1976; O'Keefe *et al.* 1998; Usrey & Reid, 2000; marmoset: Kremers *et al.* 1997; White *et al.* 1998; squirrel monkey: Usrey & Reid, 2000). It has been hypothesized that M and P cells support distinct extrastriate visual pathways, based upon differences in physiological signatures and upon their separate projection pathways to V1 and within V1 (see DeYoe & Van Essen, 1988; Livingstone & Hubel, 1988; Merigan & Maunsell, 1993; Casagrande & Kaas, 1994 for review). For example, the greater sensitivity of P cells to chromatic contrast (in macaque monkeys and marmosets) and to higher spatial frequencies (in all primate species examined) has been linked to the processing of detail and colour while the greater sensitivity of M cells to higher temporal frequencies has been linked to motion perception (DeYoe & Van Essen, 1988; Livingstone & Hubel, 1988).

Few studies, however, have examined the response properties of K LGN cells, especially in simian primates. K LGN cells have been studied in the most detail in the nocturnal prosimian bush baby (*Galago crassicaudatus*) (Norton & Casagrande, 1982; Irvin *et al.* 1986, 1993; Norton *et al.* 1988). In contrast to M and P cells, K cells in bush babies were found, on average, to have larger receptive fields and slower orthodromic and antidromic conduction velocities. Like cat W cells, bush baby K cells (referred to earlier as W-like) also appeared to be heterogeneous as a group; some could not be driven well by grating stimuli or were only poorly driven by such stimuli. Other bush baby K cells, however, were unlike the 'sluggish' cat W cells, and responded briskly to gratings; they exhibited contrast sensitivity functions whose resolution levels lay intermediate between those of the average M or P cell (Norton *et al.* 1988).

Only recently has there been an effort to examine the response properties of K cells in any simian primate (Martin *et al.* 1997; White *et al.* 1998; Solomon *et al.* 1999). Studies of K cells in the diurnal New World marmoset monkey revealed one population of K cells that appeared to receive input from blue-ON ganglion cells suggesting involvement of this pathway in the processing of chromatic information (Martin *et al.* 1997; White *et al.* 1998). Since K cells send axons to the CO blobs of V1, the latter result is consistent with the proposed role of CO blob cells in chromatic processing (Livingstone & Hubel, 1988), although recent studies in primate V1 conflict with earlier reports and suggest that CO blob cells are not unique in their selectivity for chromatic stimuli (Lennie *et al.* 1990; DeBruyn *et al.* 1993; Edwards *et al.* 1995; Leventhal *et al.* 1995). Because bush babies have only a single cone type, lack blue cones and also have well-defined CO blobs, K cells and their CO blob targets probably perform some more universal visual function than the processing of chromatic signals or perform more than one role across species (Wikler & Rakic, 1990; Casagrande & Kaas, 1994; Jacobs *et al.* 1996). Regardless, given the paucity of information available on K cell physiology, a key objective of the present study was to proceed by analogy to previous work on M and P cells and put together a physiological profile of this class of cells that might be linked to particular perceptual attributes.

Our aim for the present study was to characterize fully the receptive field properties of K LGN cells in the nocturnal simian owl monkey and compare K cell properties to those of M and P cells. Owl monkeys, like prosimian bush babies, have only one cone type and lack blue cones entirely, and like marmosets, are New World simian primates (Wikler & Rakic, 1990; Jacobs *et al.* 1993, 1996). Owl monkeys offered us several other advantages. First, with the exception of macaque monkeys, the visual systems of owl monkeys have been studied in the most detail (for review see Casagrande & Kaas, 1994). Second, owl monkeys have well-developed LGNs with simple laminar patterns consisting of two P layers, two M layers and at least three well-defined K layers. Finally, the axon structure and cortical target cells of K LGN cells in owl monkeys have been studied in detail (Ding & Casagrande, 1997). Some of the results reported here were presented previously in abstract form (Xu *et al.* 1999).

METHODS

General preparation

Conventional extracellular recording techniques were employed to examine the receptive field properties of LGN neurons in nine adult owl monkeys (*Aotus trivirgatus*). These monkeys were a gift from the USAID Malaria Vaccine Development Program. We recorded directly from LGN cells in seven owl monkeys. In the remaining two monkeys recordings were made from LGN cell afferent axons in V1 where intrinsic neuronal activity was inhibited ('silenced') by the $GABA_A$ agonist muscimol (Chapman *et al.* 1991; Boyd *et al.* 1998). All monkeys were handled according to the National Institutes of Health Guide for the Care and Use of Animals under an approved protocol from the Vanderbilt University Animal Care and Use Committee. Animals were pre-medicated with injectable atropine (0·1 mg kg^{-1}), acepromazine (0·5–1 mg kg^{-1}) and dexamethasone (2 mg kg^{-1}). Anaesthesia was induced with an intramuscular injection of ketamine HCl (8–12 mg kg^{-1}) and mask inhalation of Isoflurane. Animals were maintained with these anaesthetics while a cannula was inserted into the femoral vein of one hind-limb for subsequent delivery of anaesthetic and neuromuscular blocking agents. Anaesthesia was then maintained with injections of ketamine for the remainder of the surgical manipulations. After a cannula was placed in the trachea, the animals were mounted in a stereotaxic apparatus, the scalp was reflected on the midline and stainless-steel screws were inserted in the skull over the frontal lobe for recording EEGs to monitor general levels of arousal. Neuromuscular blockade was initiated by I.V. injection of 1–1·5 mg kg^{-1} vecuronium bromide (Norcuron). Animals were artificially ventilated with a mixture of 75% N_2O, 23·5% O_2 and 1·5% CO_2 delivered at a rate of 28–35 strokes min^{-1} with a volume of about 15 ml to maintain the peak end tidal CO_2 level at 4%. Anaesthesia and neuromuscular blockade were maintained by intravenous infusion of sufentanil citrate (Sufenta: 12–15 μg kg^{-1} h^{-1}) and vecuronium bromide (0·2 mg kg^{-1} h^{-1}) mixed in 5% dextrose lactated Ringer solution delivered at a rate of about 2·7 ml h^{-1}. In order to ensure that adequate levels of anaesthesia were maintained, heart rate, end-tidal CO_2 and EEGs

were monitored continuously in the presence of the neuromuscular blocker. If the animal exhibited any signs that the anaesthesia levels were inadequate (fluctuating heart rate or low voltage fast EEG records), the percentage of Sufenta in the infusion line was immediately increased.

For LGN recording, a small craniotomy (4 mm × 5 mm) was made over the location of LGN according to stereotaxic coordinates established previously and the dura reflected. The brain was protected with a layer of agar. After the electrode was inserted into the brain, the opening in the skull was covered with an additional layer of paraffin wax to ensure recording stability. For recordings that were to be made from 'silenced' V1, holes were drilled directly over the area centralis representation in V1 in the posterior lateral cortex; the dura in the hole was incised. Initially, the receptive field properties of one or two cortical cells in V1 were analysed. The electrode was then withdrawn and 25–50 μl of 50 mM muscimol was applied to the exposed cortex for 5–10 min to silence cortical cellular activity. The cortical surface was then rinsed with saline before the craniotomy was sealed (Chapman *et al.* 1991; Boyd *et al.* 1998). Muscimol was reapplied to the cortical surface as soon as there were signs of recovery of neural activity. Generally cortical neural activity did not show any signs of recovery during the typical duration, less than 4 h, of one penetration in cortex. LGN axons could be distinguished from cortical cells based upon their generally higher spontaneous activity, monocular responses and vigorous responses to flashing spots and rapidly moving stimuli. At the end of each penetration electrolytic lesions were made to mark cells so that their locations could be reconstructed relative to laminar and compartmental (CO blob or interblob) borders.

Pupils were dilated with atropine eye drops (1% ophthalmic atropine sulfate). Individually fitted clear gas-permeable contact lenses were used to render the retina conjugate with the viewing screen 57 cm distant. In some animals, lenses with 3 mm artificial pupils were used. Retinal landmarks (optic disk and area centralis) were projected onto the plotting screen with the aid of a reversible ophthalmoscope. The electrode was then lowered into the brain using a microdrive, and responses to visual stimuli were monitored until characteristic LGN responses were found. During physiological recording, EEG, ECG, end tidal CO_2 level and rectal temperature were monitored and maintained at appropriate levels.

Recording, stimulation and data acquisition

Commercially made Parylene-coated tungsten electrodes (FHC Inc., Bowdoinham, ME, USA) with an impedance of 5–10 MΩ were used to record from LGN cells. Well-isolated units were used to trigger standard pulses, which could be played over the audio monitor and counted by a computer that also controlled the presentation of stimuli.

The receptive fields of each unit were initially plotted by manually controlled stimuli displayed on the tangent screen, with eye dominance determined and the receptive field boundaries drawn. The receptive field centres and surrounds were identified as either ON, OFF or ON–OFF. In addition, any strong suppressive effect of the surround on the centre was noted. The horizontal and vertical extent of the receptive field centre was measured on a plotting table using a small flashing spot. The average horizontal and vertical extent of the receptive field centre was taken as the diameter of the receptive field centre. We also qualitatively differentiated cells into sustained and transient categories according to their response to stationary contrast stimuli presented for 5–10 s within the centre of the receptive field. Units that exhibited above spontaneous maintained discharge during this period were categorized as sustained.

Stimuli consisted of drifting sine-wave and counterphase gratings presented at different spatial and temporal frequencies, contrasts and orientations, and phases in the case of counterphase gratings. Stimuli were generated by an image-processing board (Pepper PRO 1280) with a capacity of 1024 pixels × 1280 pixels by 8 bits of modulation and presented on a cathode ray tube (CRT) screen that subtended an angle of 10 deg with a background luminance of 110 cd m^{-2}. Given that owl monkeys have a rod-dominated retina, we examined to see if our measurements using these luminance levels differed depending upon whether we used a 3 mm pupil or not. No differences were found. For cells with strong suppressive surrounds, stimuli were presented within a 4 deg window instead of the full 10 deg screen. Cells were tested with spatial frequencies ranging from 0·1 to 9·6 cycles deg^{-1}, temporal frequencies ranging from 1 to 32 Hz at the optimal spatial frequencies, and contrasts ranging from 3 to 56% at optimal spatial and temporal frequencies. Linearity was tested using different phase angles of the counterphase sine-wave gratings stepped through the receptive field such that the cell's responses were sampled at all positions within the centre and surround at least once. The initial linearity test was run with spatial, temporal and orientation parameters optimized for the cell at moderate contrast (28%). Next the cell was re-tested at double its preferred spatial frequency. If the cell still responded adequately it was retested at 3 times the optimal spatial frequency, and so forth, until the cell no longer responded. By increasing the spatial frequency we could ensure that non-linearities in spatial summation would be reliably detected if present (Hochstein & Shapely, 1976; Derrington & Lennie, 1984).

Data were collected by a generic PC-386. The primary data analysis tool was construction of 2 s, 128 bins s^{-1} post-stimulus time (PST) histograms. The interleaved histogram technique of Henry *et al.* (1973) with randomization was adopted to reduce artifacts from the inherent non-stationarity of the visual system. A stimulus set was specified and comprised each measuring condition as well as a null condition (a blank screen at the mean luminance of the gratings) to assess the maintained discharge. Each element in the stimulus set was presented once in a random order with a 1 s interval of blank screen between each presentation. Presentation of the set was then repeated in a random order until each stimulus condition had been tested completely (5–10 times). With 4 s presentation periods, data are based on 20–40 s of averaging for each condition. The PST histograms for each cell were Fourier transformed, and the fundamental (F1) and second harmonic (F2) components of the response were analysed. Data were plotted with IGOR 3.1 (WaveMetrics, Inc.) software. The following receptive field properties were measured for each cell: peak spatial frequency and cut-off, peak temporal frequency and cut-off, response to stimulus contrast and linearity of spatial summation. In addition, we determined orientation selectivity for each cell tested and all remaining tests were done with the grating stimuli set to the preferred orientation if one existed. Data on the orientation selectivity of LGN cells in owl monkey will be submitted for publication separately. If the cell exhibited no orientation selectivity then all tests involved vertically oriented drifting gratings.

We examined linearity of spatial summation with counterphase gratings in all the cells that responded well to drifting gratings. The ratio of the mean amplitude of the second harmonic (averaged across all spatial phases) to the amplitude of the fundamental at the best phase was used as an index of non-linearity (Hochstein & Shapley, 1976; Derrington & Lennie, 1984). An index value greater than 1·0 indicates a substantial non-linearity. In the present study, cells with 2nd harmonic (F2)/1st harmonic (F1) ratios of $< 1{\cdot}0$ at all spatial frequencies tested were classified as linear cells. Cells with

F2/F1 ratios > 1·0 at any one of the spatial frequencies tested were classified as non-linear cells.

Spatial and temporal frequency peaks were defined as the frequencies at which cells exhibited the highest first harmonic response. Cut-offs were determined by extrapolating the high-frequency limb of the curves (*vs.* log frequency) to control levels determined from responses to the blank control screen (baseline).

Several measures of contrast sensitivity were compared. Threshold contrast was determined by extrapolating to baseline (*vs.* log contrast). Contrast gain was determined based upon the slope of the linear portion of the contrast–response curve (*vs.* log contrast) where responses were well above threshold. In addition, we attempted to fit contrast–response curves with a hyperbolic function in the form of:

$$\text{Response}\,(C) = R_{\max}(C^n/(C^n + {C_{50}}^n)),$$

where $R_{\max}$ is the maximum response rate, C_{50} is the contrast required for half-maximal response, and the exponent n is the rate of change (Albrecht & Hamilton, 1982). Such hyperbolic fits were useful only in those cells that exhibited response saturation. In this group we also compared C_{50} values obtained from these curve fits.

Statistical analysis

Statistical comparisons of receptive field properties across the K, P and M groups were done by one-way ANOVA with *post hoc* mean difference tests (Tukey and LSD tests), provided that the data did not violate the prerequisite of variance homogeneity across groups. For groups with both unequal variances and unequal samples, we used instead the Kruskal-Wallis test, which is a non-parametric procedure commonly advocated as an alternative of the ANOVA (Zar, 1999). In the latter case, a Mann-Whitney U test was used for between group comparisons. Alpha levels of $P \leqslant 0{\cdot}05$ were considered significant.

Histological procedures

The position of each recorded cell or axon was noted by the depth indicated on the microdrive. Electrolytic lesions (5 μA × 5 s) were made to mark the location of electrode tracks (see Fig. 1). At least two electrolytic lesions were made on each electrode penetration to aid in reconstruction of the track and to calculate tissue shrinkage. At the termination of each experiment, the animal was deeply anaesthetized with an overdose of Nembutal (sodium pentobarbital) and perfused transcardially with a saline rinse followed by fixation with 0·1% glutaraldehyde and 3% paraformaldehyde in 0·1 M phosphate buffer. The brain was removed and cryoprotected overnight in a solution containing 30% sucrose in 0·1 M phosphate buffer. It was then frozen and cut into 50 μm slices. To locate the LGN cells recorded, alternate sections of the LGN were stained for Nissl bodies, CO or immunostained for calbindin-D28k. CO staining was performed using the method described by Boyd & Matsubara (1996).

For LGN afferent axons in V1, K axons can be distinguished anatomically since they terminate within cortical layers III and I, while M and P axons terminate within the upper and lower halves of cortical layer IV, respectively (see Ding & Casagrande, 1997). To identify cortical layers alternate V1 sections were stained for Nissl bodies and CO, respectively. LGN axon types were classified based upon the laminar position established via reconstructions of the electrode tracts.

Calbindin immunostaining was used to identify the K layers, which are numbered K1–K4 beginning with K1 located between the optic tract and the first M layer (see Fig. 1). Only those axons or cells that could be located histologically with confidence were included for further data analysis.

Calbindin immunostaining was performed using a rabbit polyclonal antibody (Swant CB-38). Before being placed in the primary antibody, the sections were placed in 0·3% H_2O_2 for 30 min followed by three rinses in 0·1 M Tris-buffered saline (TBS; pH 7·4). Sections were then incubated for 1 h in blocking buffer consisting of 10% normal donkey serum, 1% bovine serum albumin and 0·1% Triton X-100 in TBS. Then the sections were placed in primary antibody diluted 1:5000 in antibody buffer consisting of 10% normal horse serum, 0·2% bovine serum albumin and 0·2% Triton X-100 in TBS. Sections were incubated overnight in the primary antibody and then rinsed 3 times in TBS before being placed in the secondary antibody. The secondary antibody (biotinylated donkey anti-rabbit (Chemicon)) was diluted at 1:200 in antibody buffer. Sections were incubated in secondary antibody for 2 h, rinsed 3 times in TBS and placed in an avidin–biotin complex (Standard Elite ABC kit, Vector) prepared in TBS. After 2 h the sections were rinsed 3 times with TBS and the calbindin immunoreactivity was visualized by placing the sections into a solution containing 50 mM imidazole, 25 mM nickel ammonium sulfate, 0·01–0·02% 3,3-diaminobenzadine and 0·0003% H_2O_2 in 0·05 M TBS. Sections remained in this solution until labelled cells were visible and the reaction product was quite dark (usually 15–20 min).

RESULTS

We recorded from 133 LGN cells and 10 LGN afferent axons in silenced V1 with eccentricities ranging from 2·8 to 31·3 deg. All LGN axons recorded from silenced V1 had eccentricities of less than 10 deg. From this total population 38 K units (36 cells and 2 axons), 45 P cells and 34 M units (29 cells and 5 axons) could be assigned with confidence to specific layers based upon histological reconstructions.

Receptive field structure and size

Twenty (53%) of the 38 K units analysed gave a sustained response to a stationary stimulus held in the receptive field centre for at least 5 s. The remaining 18 (47%) responded transiently. Twenty-three K units exhibited typical centre–surround receptive fields either ON centre with an OFF surround or the converse. Fifteen of the K units had either strong suppressive surrounds, ON–OFF surrounds or no clear surrounds. Thirteen K units (34%) were poorly driven by grating stimuli, but responded well to flashing spots or single light bar stimuli moved manually. Of the 13 K cells that did not respond to gratings, 2 appeared to respond only to changes in luminance and, although this impression was not tested quantitatively, these cells seemed to respond very much like the 'luminance units' described in the cat retina by Barlow & Levick (1969). In addition, two other K cells seemed to have unusually long onset latencies to flashing spots of light.

Thirteen (38%) of the 34 M units analysed responded in a sustained manner and the remainder responded transiently to a stationary stimulus of appropriate contrast. In contrast to the K and M populations, the majority (71%) of P cells responded in a sustained fashion. Ninety per cent of the P and M units showed standard centre–surround receptive fields; the remainder showed either weak or unclear surrounds or suppressive surrounds. Also, in contrast to the

K population, only four P cells (9%) and two M cells (6%) responded poorly to grating stimuli although all of these cells responded briskly to flashing spots or moving bars of light.

Since one property reported to characterize cat W cells is that of sluggishness (see Sur & Sherman, 1982) we compared the peak response rates with optimal stimulus conditions for those K, P and M cells that responded to gratings. As reported by Usrey & Reid (2000), owl monkey LGN cells tend to show low overall peak responses. No statistical differences ($P = 0{\cdot}27$) were found between K, M and P cells in peak responses to spatial and temporal frequencies at moderate contrast (28%): K cells, $10{\cdot}6 \pm 1{\cdot}0$ spikes s^{-1} (mean ± S.E.M.; $N = 24$), M cells, $12{\cdot}4 \pm 1{\cdot}0$ spikes s^{-1} ($N = 32$); and P cells $10{\cdot}2 \pm 1{\cdot}0$ spikes s^{-1} ($N = 33$).

In all three LGN cell classes receptive field centre size tended to increase with eccentricity, but this relationship was least clear for the K population where there was a large

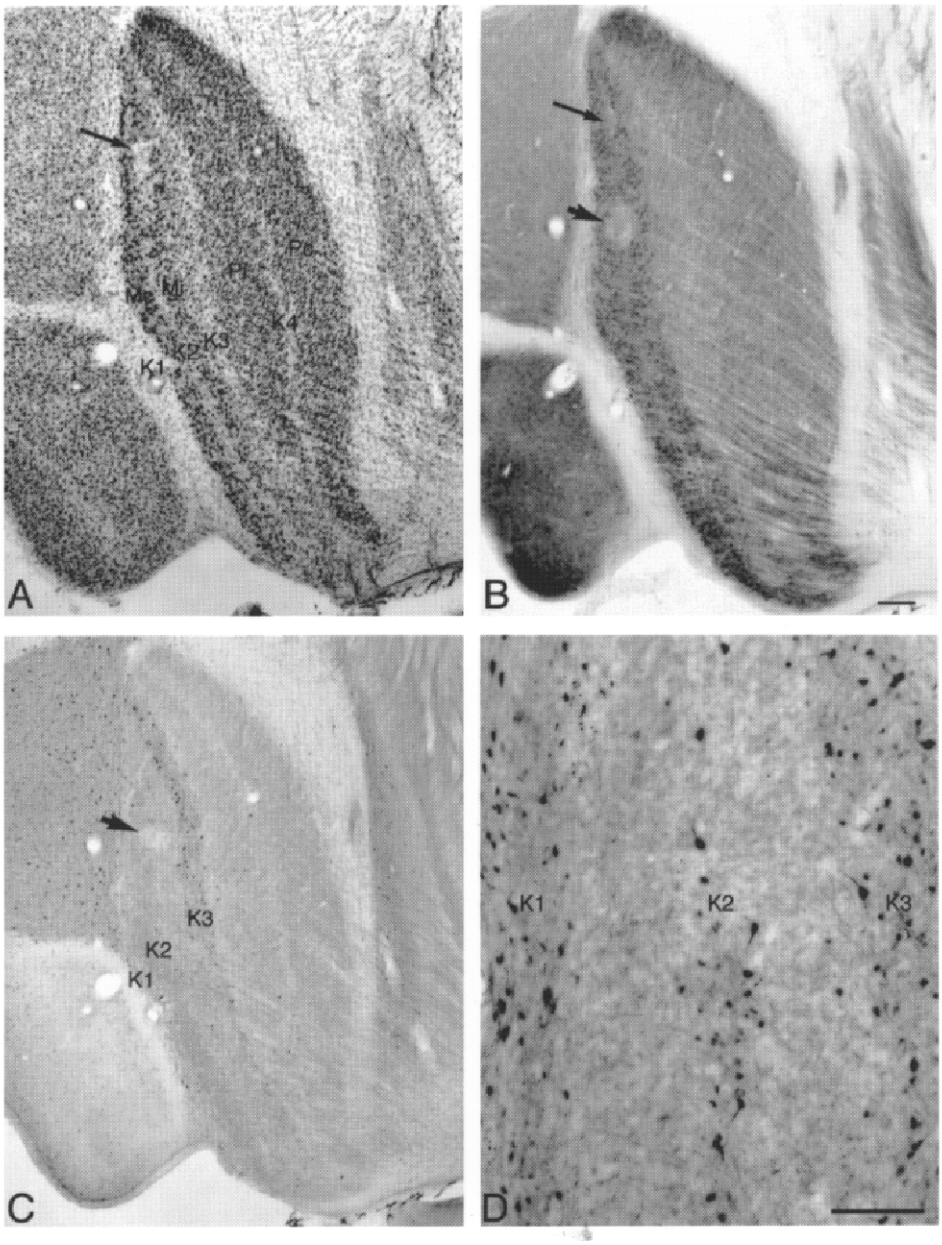

Figure 1. Histological reconstruction of recording sites

Photomicrographs of adjacent parasagittal LGN sections showing lesions in sections stained for Nissl bodies (*A*), CO (*B*) and calbindin-D28k (*C* and *D*). Calbindin-D28k labels cells mainly in layers K1, K2 and K3. Calbindin-labelled cells in K4 are sparse. The arrow and arrowhead in *B* indicate a pair of lesions located in the contralateral M layer (arrowhead) and in layer K2 (arrow) that mark a single electrode penetration. The arrows in *A* and *B* point to the same lesion; arrowheads in *B* and *C* point to the same lesion. *D* shows a higher power photomicrograph of the distribution of K cells immunostained for calbindin-D28k in K layers K1–K3 in another case. Scale bar in *B*, 200 μm and also applies to *A* and *C*; in *D*, 100 μm.

degree of scatter at all eccentricities. Figure 2 shows the relationship between receptive field centre size and eccentricity for the subset of the K (14), P (19) and M (18) cells where centre boundaries were unambiguous. For this population, average receptive field centre diameter was $1{\cdot}05 \pm 0{\cdot}25$ deg for K cells, $0{\cdot}87 \pm 0{\cdot}11$ deg for P cells and $0{\cdot}92 \pm 0{\cdot}13$ deg for M cells.

Linearity of spatial summation

In cats the major feature that is used to distinguish X and Y retinal ganglion and LGN cells is linearity or non-linearity of spatial summation (Enroth-Cugell & Robson, 1966; Hochstein & Shapley, 1976). According to Hochstein & Shapley (1976) the identification of a cell as an X cell on the basis of linear summation requires not only a strong dependence on spatial phase and response at the fundamental modulation frequency, but also that spatial phase dependence be demonstrated at higher than the cell's preferred spatial frequency. This is because Y cells can exhibit a strong spatial phase dependence and respond quite well at the fundamental modulation frequency if the grating is presented at a low spatial frequency. Therefore, we also examined for spatial phase dependence both at the preferred spatial frequency of the cell and at least 2 × the preferred frequency. Cells were considered to respond linearly if they showed a clear null F1 response. Also, if the F2 response became dominant over the F1 response we classified the cell as non-linear (Hochstein & Shapley, 1976). In Y cells the F2 component was found to be phase insensitive. We calculated the F2/F1 response ratio as an index of non-linearity. In cats, X cells were always found to have a non-linearity index of less than 1·0 while for Y cells this index was found to be greater than 1·0 (Hochstein & Shapley, 1976).

We found that all K ($N = 17$), P ($N = 32$) and all but one M ($N = 27$) unit could be classified as linear according to the above described criteria. Figure 3 shows examples of the spatial phase dependence in the responses of different LGN cells and provides a summary histogram showing the non-linearity indices of all cells.

The K cell shown in Fig. 3*A* was tested at its optimal spatial frequency of 0·8 cycles deg^{-1}. The peaks of the F1 responses are much higher than average F2 responses at all phases outside of the null points. This cell exhibited a non-linearity index of 0·21. Nulls are clearly evident at phase positions −120 and 60 deg. Figure 3*B* shows the responses of the same cell tested at 2 × the optimal spatial frequency. As would be expected the F1 responses decrease as the spatial frequency is increased beyond the cell's preferred frequency but at no point is the average F2 response higher than the F1 response. Even at 2 × the preferred spatial frequency, this cell still exhibits clear evidence of a null. All P cells and all but one M cell showed clear evidence of spatial linearity. The spatial phase responses of a typical M cell are shown in Fig. 3*C*. In this example the cell was tested at 2 × its preferred spatial frequency. The F1 response curve exhibits nulls at −90 and 90 deg. At the peak responses of this cell the F1 curve is always higher than the F2 curve. Only one M cell showed any indication of non-linearity (Fig. 3*D*). In this cell the peak F2 responses are higher than the F1 response. However, unlike cat Y cells this cell shows evidence of phase dependence.

Figure 3*E* shows a summary distribution of the non-linearity indices for all cells in the population tested at their optimal or close to optimal spatial frequencies. Only one M cell (also shown in Fig. 3*D*) exhibited an index of greater than 1·0 suggesting spatial non-linearity. The distributions of the non-linearity indices for the other cells show no clear trends that correlate with cell class. The majority of K, M and P cells show non-linearity indices of $< 0{\cdot}4$ with a peak for each of the populations around 0·2.

Spatial and temporal resolution

Spatial and temporal frequency tuning curves and responses to contrast are shown for representative K, P and M cells in

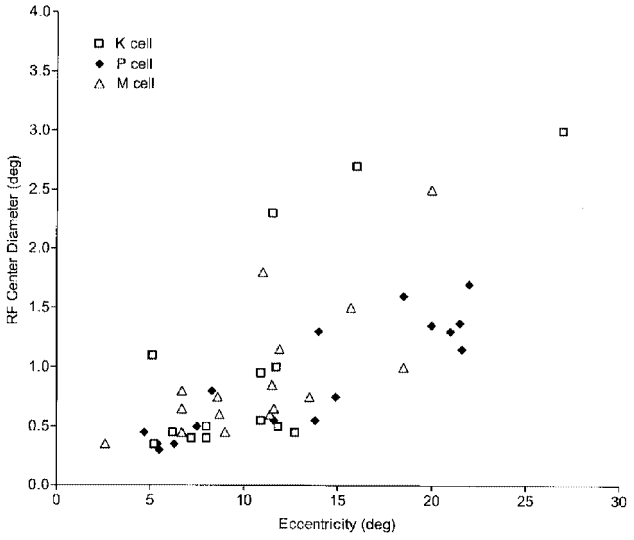

Figure 2. Receptive field centre diameter *vs.* eccentricity

K, P and M cells (represented by □, ◆ and △, respectively) show increases in receptive field centre size with eccentricity. K cells, however, show more scatter.

Figs 4, 5 and 6, respectively. The K cell shown in Fig. 4*A* exhibited a peak spatial frequency at about 0·8 cycles deg^{-1} and a high spatial frequency cut-off at around 6 cycles deg^{-1}. Typical of all K cells tested, this K cell showed a broad band-pass tuning curve with a sharper drop-off in response to higher than lower frequencies. As shown in Fig. 4*B*, this K cell responded to temporal frequencies over a broad range from 1·0 Hz (the lowest temporal frequency tested) to 6·0 Hz with a clear peak at 2 Hz. The contrast–response function for this same K cell is shown in Fig. 4*C*. The extrapolated contrast threshold for this cell is about 2·5%, and its contrast gain (the slope for the linear segment of the rising phase) is 29 spikes s^{-1} per log contrast %.

Spatial and temporal tuning curves for a representative P cell are shown in Fig. 5. Unlike K and M cells most P cells exhibited symmetrical band-pass spatial frequency tuning curves. This cell showed a peak spatial frequency response at 0·8 cycles deg^{-1} and a cut-off around 6·4 cycles deg^{-1} (Fig. 5*A*). Like the K cell shown in Fig. 4, this P cell had a peak temporal frequency at 2·0 Hz but a higher cut-off at 10 Hz. The contrast–response curve for this P cell is shown

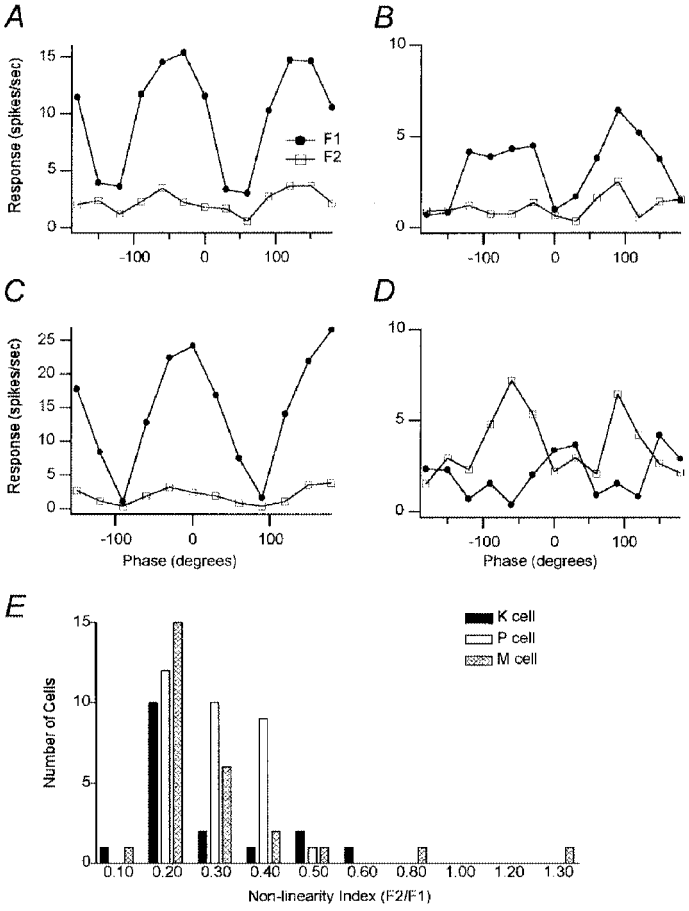

Figure 3. Linearity of spatial summation

The first harmonic component (F1) is shown by ● and the second harmonic component (F2) by □. *A*, an example of a K cell tested with a phase angle range (from −180 to 180 deg) in 12 steps at its optimal spatial frequency (SF 0·8 cycles deg^{-1}), optimal temporal frequency (TF 2 Hz) and moderate contrast (28%). The F1 curve had null positions around −120 and 60 deg. *B*, the same K cell tested at 2 × the optimal SF (SF 1·6 cycles deg^{-1}). Its F1 responses decreased, but the peaks of the F1 curve were still higher than the average F2 curve across all phase angles. *C*, phase tuning curve for an M cell at 2 × its optimal spatial frequency (SF 0·8 cycles deg^{-1}), optimal temporal frequency (TF 2 Hz) and moderate contrast (28%). The peaks of the F1 curve were higher than the average F2 curve at all phase angles. The F1 curve had null positions around −90 and 90 deg. *D*, only one M cell exhibited any evidence of spatial non-linearity. This cell was tested with a global phase angle range (from −180 to 180 deg) in 12 steps at its optimal spatial frequency (0·6 cycles deg^{-1}), optimal temporal frequency (2 Hz) and moderate contrast (28%). Average F2 responses across all phase angles except at the centre of the field are higher than F1 responses with a ratio of F2/F1 greater than 1·0 at the peaks. *E*, non-linearity index (F2/F1) histograms of K, P and M cells. Most K, P and M cells have a non-linearity index of less than 0·4. Out of 76 cells (K = 17, P = 32, M = 27), one M cell had an index greater than 1·0 suggestive of spatial non-linearity.

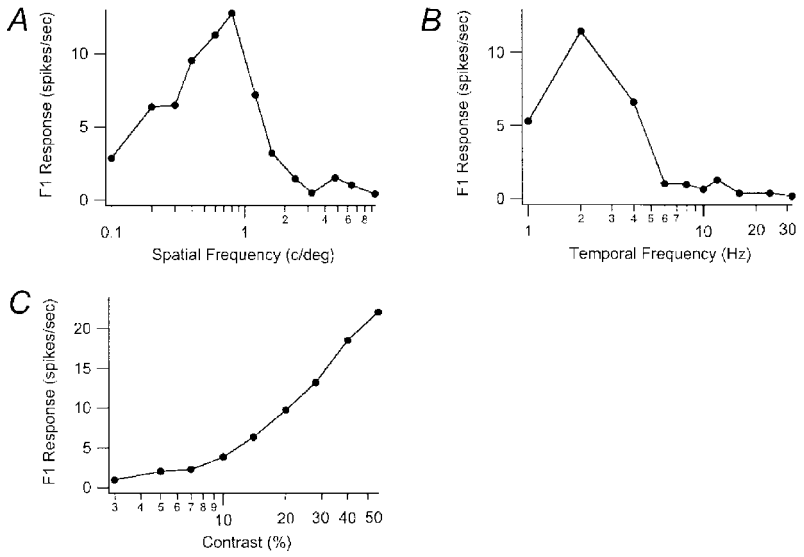

Figure 4. K cell spatial frequency, temporal frequency and contrast tuning curves

The F1 response curves for one K cell are shown for different spatial frequencies (in cycles deg^{-1}) in *A* and different temporal frequencies (in Hz) in *B*. This cell had a SF peak at 0·8 cycles deg^{-1} and a cut-off around 6 cycles deg^{-1}. The peak TF was 2 Hz and the cut-off was around 6 Hz. The contrast response curve is shown in *C*.

in Fig. 5*C*. It shows a sigmoidal shape and an extrapolated threshold of around 5% contrast and a contrast gain of 29·2 spikes s^{-1} per log contrast %. Most P cells had contrast gains of less than 15 spikes s^{-1} per log contrast %, which was lower than that found in most M and K cells.

Spatial and temporal tuning curves for a representative M cell are shown in Fig. 6. Unlike K and P cells, some M cells did not exhibit a low spatial frequency roll-off as shown in Fig. 6*A*. This cell had a peak spatial frequency of 0·2 cycles deg^{-1} and spatial frequency cut-off of 6 cycles deg^{-1}. This cell also responded well to all temporal frequencies from 1·0 Hz (the lowest tested) to 8 Hz but still responded above background at 20 Hz. This cell's peak temporal frequency is the same as that for the K and P cells shown earlier, 2 Hz (Fig. 6*B*). The contrast–response curve for this M cell is shown in Fig. 6*C*. It shows an extrapolated threshold of 2·5% contrast and a contrast gain of 18·9 spikes s^{-1} per log contrast %.

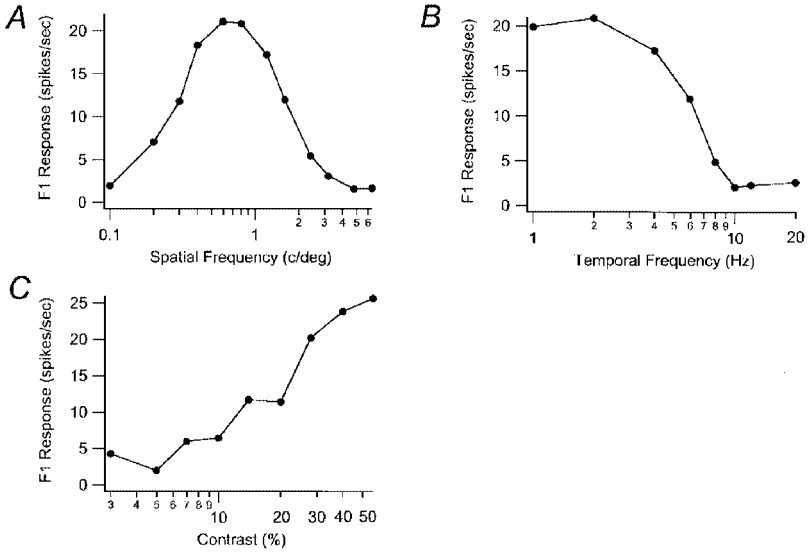

Figure 5. P cell spatial frequency, temporal frequency and contrast tuning curves

The F1 response curves for one P cell are shown for different spatial frequencies (in cycles deg^{-1}) in *A* and different temporal frequencies (in Hz) in *B*. This cell had a SF peak at 0·8 cycles deg^{-1} and a cut-off above 6·4 cycles deg^{-1}. The peak TF was 2 Hz and the cut-off was 10 Hz. The contrast response curve is shown in *C*.

Table 1. Summary of spatial and temporal resolution and contrast sensitivity values for the K, P and M populations

	Peak SF	SF cut-off	Peak TF	TF cut-off	Contrast threshold	Contrast gain
K cell ($n = 25$)	0·56 ± 0·07	3·0 ± 0·3	2·19 ± 0·17	11·3 ± 0·9	4·5 ± 0·6	17·5 ± 2·0
P cell ($n = 41$)	0·72 ± 0·06	4·5 ± 0·6	2·13 ± 0·12	9·6 ± 0·7	4·7 ± 0·6	15·0 ± 1·1
M cell ($n = 32$)	0·59 ± 0·06	3·3 ± 0·3	2·09 ± 0·13	12·5 ± 1·2	3·2 ± 0·2	18·8 ± 1·4

All values are means ± S.E.M.

Table 2. Summary of spatial and temporal resolution and contrast sensitivity values for the K, P and M cells at matched eccentricity (> 10 deg)

	Peak SF	SF cut-off	Peak TF	TF cut-off	Contrast threshold	Contrast gain
K cell ($n = 15$)	0·43 ± 0·07	2·7 ± 0·4	2·25 ± 0·25	11·2 ± 1·2	3·8 ± 0·6	17·6 ± 2·8
P cell ($n = 27$)	0·69 ± 0·06	4·0 ± 0·4	1·96 ± 0·11	9·1 ± 0·8	5·0 ± 0·8	14·5 ± 1·3
M cell ($n = 16$)	0·43 ± 0·06	3·1 ± 0·51	2·06 ± 0·17	14·9 ± 2·0	2·9 ± 0·3	18·2 ± 1·4

Table 1 provides the mean ± S.E.M. spatial and temporal resolution values for each population of cells which included a total of 25 K, 41 P and 32 M units. Statistical comparisons were confined only to the 15 K, 27 P and 16 M cells (Table 2) at roughly matched eccentricities (> 10 deg). The histograms in Figs 7–9 compare the eccentricity-matched populations for each parameter measured. As can be seen in Table 2 and Fig. 7 K, P and M cells show broad overlapping ranges of peak and cut-off spatial frequencies. A one-way ANOVA comparison of the populations at matched eccentricities revealed significant differences in peak spatial frequencies and cut-offs ($P = 0·008$ and 0·05, respectively). A *post hoc* mean test showed that the P cells had significantly higher peak spatial frequencies than K or M cells ($P = 0·02$ and 0·03, respectively); the mean peak spatial frequencies for K and M cells did not differ ($P = 0·99$). P cells differed significantly from M cells in their spatial frequency cut-offs ($P = 0·05$). Although K cells tended to have lower mean spatial cut-offs than P cells, this trend did not reach significance (P *vs.* K, $P = 0·26$; M *vs.* K, $P = 0·73$).

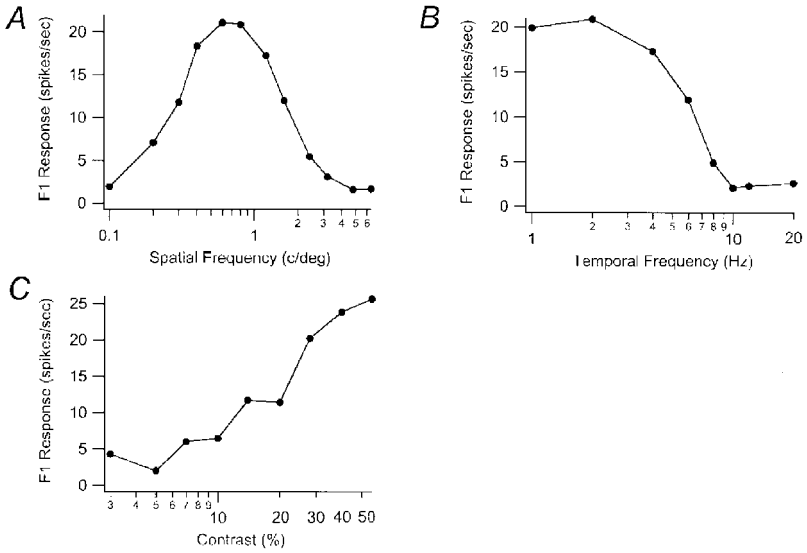

Figure 6. M cell spatial frequency, temporal frequency and contrast tuning curves

The F1 response curves for one M cell are shown for different spatial frequencies (in cycles deg^{-1}) in *A* and different temporal frequencies (in Hz) in *B*. This cell had a SF peak at 0·2 cycles deg^{-1} and a cut-off around 6 cycles deg^{-1}. The peak TF was 2 Hz and the cut-off was above 20 Hz. The contrast response curve is shown in *C*.

Interestingly, as shown in Fig. 7*A*, the K cells' peak spatial frequency distribution appeared to have two modes suggesting that K cells have subclasses.

Figure 8 compares the peak and cut-off temporal frequencies for K, P and M cells. Mean values are given in Table 2. As can be seen in Fig. 8*A*, K, P and M cells have very similar temporal frequency peak distributions with most cells preferring 2·0 Hz. Figure 8*B* shows that K cells have temporal frequency cut-offs that lie between those of P and M cells although here again the populations show broad areas of overlap. Temporal frequency cut-offs were found to differ significantly between the three groups (Kruskal-Wallis test, $P = 0{\cdot}003$). This difference can be accounted for by differences between P and M cells ($P = 0{\cdot}001$) since Mann-Whitney U tests showed that the K cell population did not differ from either the M ($P = 0{\cdot}22$) or P ($P = 0{\cdot}07$) populations. As can be seen, the temporal resolution values of K cells lie between those of P and M cells.

It is also noteworthy that, as demonstrated for K cells in the peak spatial frequency domain, M cells exhibit double peaks indicative of two modes in both spatial and temporal frequency cut-offs (Figs 7*B* and 8*B*). The double peaks seen in the M distributions also may hint at the existence of subclasses.

Figure 9 compares contrast threshold values (*A*) and the contrast gain values (*B*) for each of the populations; mean values are shown in Table 2. Contrast thresholds of M cells were significantly lower than those of P cells (Mann-Whitney U test, $P = 0{\cdot}05$). K cells did not differ significantly from M or P cells ($P = 0{\cdot}26$ and $0{\cdot}45$). M cells exhibited significantly higher average contrast gains than P cells (Mann-Whitney U

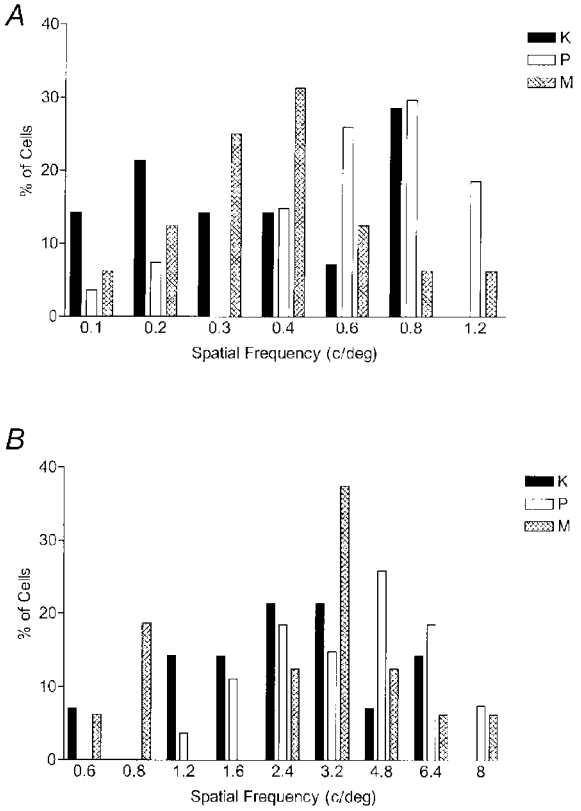

Figure 7. Histograms of peak spatial frequencies and cut-offs for K, P and M cells with matched eccentricities of > 10 deg

A, the peak spatial frequencies of K, P and M cells are represented by filled, open and cross-hatched bars, respectively. The mean peak SF was $0{\cdot}43 \pm 0{\cdot}07$ cycles deg^{-1} for K cells ($n = 15$), $0{\cdot}69 \pm 0{\cdot}06$ cycles deg^{-1} for P cells ($n = 27$) and $0{\cdot}43 \pm 0{\cdot}06$ cycles deg^{-1} for M cells ($n = 16$). P cells had a significantly higher peak SF than K and M cells (ANOVA and *post hoc* mean tests; $P \leqslant 0{\cdot}05$), but K and M cells were not significantly different. *B*, the mean SF cut-off was $2{\cdot}7 \pm 0{\cdot}4$ cycles deg^{-1} for K cells, $4{\cdot}0 \pm 0{\cdot}4$ cycles deg^{-1} for P cells and $3{\cdot}1 \pm 0{\cdot}5$ cycles deg^{-1} for M cells. SF cut-off differed significantly between P and M cells ($P \leqslant 0{\cdot}05$), although the cut-off for K cells did not differ significantly from P or M cells.

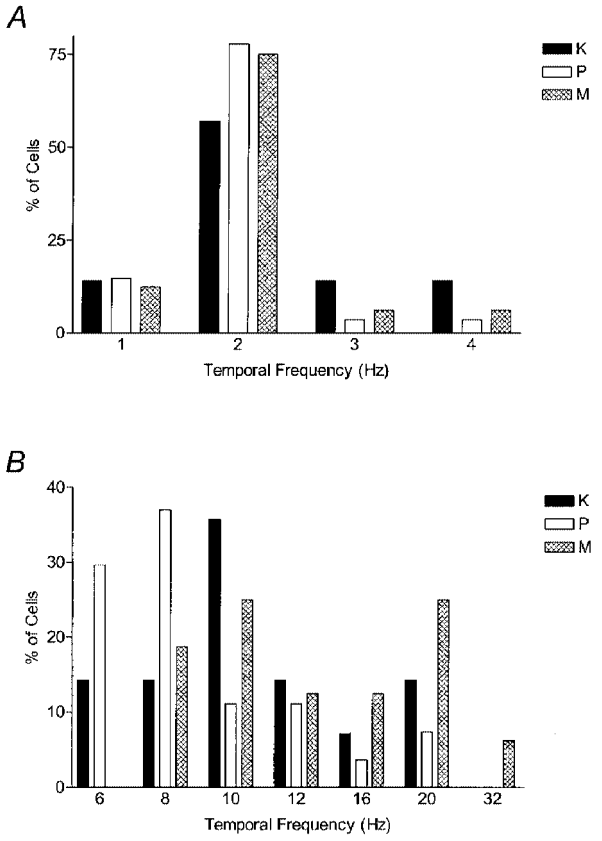

Figure 8. Histograms of peak temporal frequencies and cut-offs for K, P and M cells with matched eccentricities of > 10 deg

A, the peak temporal frequencies of K, P and M cells are represented by filled, open and cross-hatched bars, respectively. The mean peak TF was $2{\cdot}25 \pm 0{\cdot}25$ Hz for K cells, $1{\cdot}96 \pm 0{\cdot}11$ Hz for P cells and $2{\cdot}06 \pm 0{\cdot}17$ Hz for M cells. Peak TF did not differ significantly between K, M and P cells. *B*, the mean TF cut-off was $11{\cdot}2 \pm 1{\cdot}2$ Hz for K cells, $9{\cdot}1 \pm 0{\cdot}8$ Hz for P cells and $14{\cdot}9 \pm 2{\cdot}0$ Hz for M cells. K cells were not significantly different from P and M cells, but P cells had a significantly lower cut-off than M cells (Mann-Whitney U test, $P \leqslant 0{\cdot}05$).

test, $P = 0{\cdot}05$), although K cells did not differ significantly from either P or M cells ($P = 0{\cdot}48$ and $0{\cdot}53$). Thus, as with temporal resolution, the contrast characteristics of K cells seem to lie between those of M and P cells.

We also attempted to fit contrast–response curves for all the cells tested with a hyperbolic function in the form of:

$$\text{Response}\,(C) = R_{\max}\,(C^n/(C^n + {C_{50}}^n)),$$

where $R_{\max}$ is the maximum response rate, C_{50} is the contrast required for half-maximal response and the exponent n is the rate of change or contrast gain index (Albrecht & Hamilton, 1982). The contrast–response curves of the majority of M (24/32) and K cells (15/23) were well fitted by a hyperbolic function; however, the curves of most P cells (25/37) showed little response saturation and thus could not be adequately fitted by this function. For those K, P and M cells where the fit was good, the mean C_{50} differed between populations. For K cells it was $25{\cdot}9 \pm 4{\cdot}0$, for P cells $39{\cdot}0 \pm 5{\cdot}3$ and for M cells $20{\cdot}7 \pm 2{\cdot}6$. The mean C_{50} differed significantly between the three groups (ANOVA, $P = 0{\cdot}005$). The mean C_{50} of P cells was significantly different from that of either M or K cells (P *vs.* M, $P = 0{\cdot}001$; P *vs.* K, $P = 0{\cdot}03$). However, the mean C_{50} of K cells did not differ significantly from that of M cells ($P = 0{\cdot}29$).

Properties of K cells in different layers

There are four K layers in the owl monkey based upon the distribution of calbindin-labelled cells. Of these K layers, three are well developed, with K1 and K3 exhibiting the largest number of K cells (see Fig. 1*C* and *D*). Of our sample of K units, reconstructions indicated that 2 K axons in V1 were in layer 3B suggesting that they probably arose from LGN layer K3; 4 were in LGN layer K1, 11 were in LGN layer K2, 20 were in LGN layer K3 and 1 was in LGN layer K4. However, of the total sample of 38 K units, only 3 K1, 6 K2, 14 K3 cells plus the 2 K axons responded well enough to grating stimuli for quantitative measures to be made. Since our previous anatomical studies in owl monkeys showed that the different K cell layers (K1/K2 *vs.* K3) have distinct axonal termination patterns in V1 (Ding & Casagrande, 1997), we asked whether these anatomical distinctions correlated with any differences in K cell receptive field properties. As shown in Fig. 10 differences were found between the properties of cells in the different K layers. Cells in K1/K2 tended to be selective for lower spatial frequencies and higher temporal frequencies than cells in layer K3 (Fig. 10*A* and *B*). These trends were significant, however, only for the differences between temporal frequency cut-offs (Mann-Whitney *U* test, $P = 0{\cdot}05$) perhaps due to the small N value. In addition, K1/K2 cells consistently exhibited higher contrast thresholds and lower contrast gains than K3 cells (Fig. 10*C* and *D*), although this trend did not reach statistical significance. Overall, these K layer differences suggest that the ventral-most K layers, K1/K2, resemble M cells more than P cells in their spatial and temporal resolution characteristics whereas the resolution values of K3 cells tend to lie intermediate between those of P and M cells. Clearly, a larger N value will be required to confirm the trends seen.

DISCUSSION

By analogy to previous work on M and P cells, our goal was to construct a physiological profile of K cells that might be linked to particular visual perceptual attributes. We find that the spatial and temporal resolution of most K cells in the owl monkey overlap extensively those of M and P cells and that, unlike M and P cells, a large minority of K cells could not be driven by standard drifting gratings. The response of the K cell population to visual stimuli is therefore more heterogeneous than the response of either the M or P cell population. Finally, our data provide evidence that some of the heterogeneity within the K population can be accounted for by position in the LGN because cells in different K layers exhibit differences in spatial and temporal

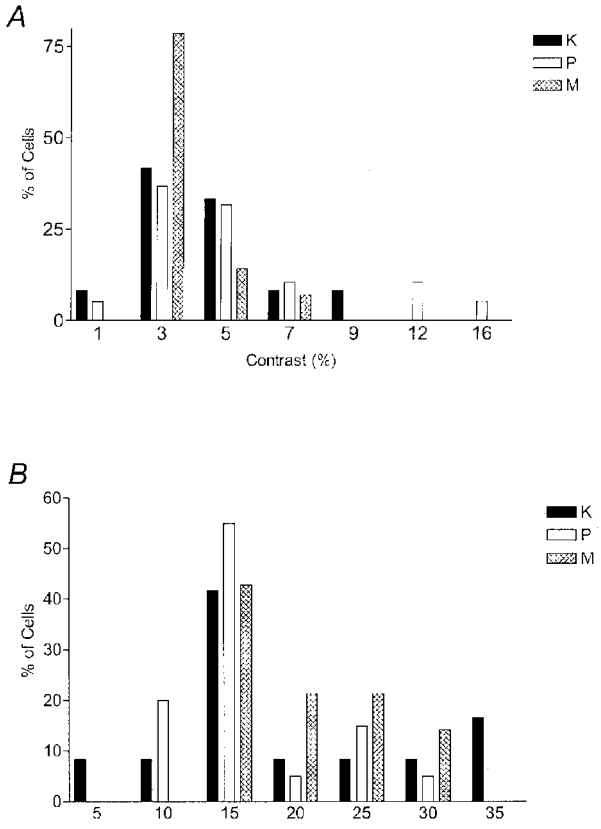

Figure 9. Histograms of contrast threshold and contrast gain for K, P and M cells at matched eccentricities of > 10 deg

A, the mean contrast threshold was $3{\cdot}8 \pm 0{\cdot}6$ for K cells, $5{\cdot}0 \pm 0{\cdot}8$ for P cells and $2{\cdot}9 \pm 0{\cdot}3$ for M cells. K cells were not significantly different from P and M cells, but M cells had a significantly lower threshold than P cells (Mann-Whitney *U* test, $P \leqslant 0{\cdot}05$). *B*, the mean contrast gains were $17{\cdot}6 \pm 2{\cdot}8$ for K cells, $14{\cdot}5 \pm 1{\cdot}3$ for P cells and $18{\cdot}2 \pm 1{\cdot}4$ for M cells. K cells were not significantly different from P and M cells, but M cells had a significantly higher gain than P cells (Mann-Whitney *U* test, $P \leqslant 0{\cdot}05$).

resolution. We will consider each of these findings in light of studies conducted by others.

Non-standard receptive field properties

A third of the K cells in owl monkeys responded poorly or not at all to drifting gratings. Less than 8% of P and M cells displayed similar response behaviour. Compared with the M and P cells, a larger proportion of K cells also were difficult to characterize with other stimuli including manually moved light bars or flashing spots of various sizes. This description of K cell responses is consistent with earlier findings in the prosimian bush baby (Norton & Casagrande, 1982; Irvin *et al.* 1986) and the New World simian marmoset (Solomon *et al.* 1999; A. J. White, S. G. Solomon & P. R. Martin, unpublished observations). The existence in owl monkeys, bush babies and marmosets of many K cells that cannot be driven by standard stimuli supports the idea that K cells are quite distinct from M and P cells. Some of the non-standard characteristics that have been reported for both simian and prosimian K cells have also been reported for cat W cells. These properties include very large and difficult-to-plot receptive fields, and non-standard centre–surround organization. Some K cells may therefore be analogous to cat W cells (Sur & Sherman, 1982; see also Norton & Casagrande, 1982).

Receptive field structure and size

Consistent with an earlier study of LGN receptive field properties in owl monkeys (Sherman *et al.* 1976), we found that M cells were, on average, more transient in their responses to appropriate standing contrast stimuli than were P cells. Approximately half the K cells we tested responded in a transient manner. We did not find a correlation between the degree of response transience and other properties of K cells, but this possibility was not examined in detail. Sustained and transient responses have been previously examined for all three cell classes only in the bush baby by Norton & Casagrande (1982) who reported that most M cells exhibited transient responses, most P cells exhibited sustained responses, and about equal numbers of K cell were sustained or transient.

Receptive field centre sizes in owl monkey tend to increase with increasing eccentricity as in the LGNs of other primates (present study; for review see Casagrande & Norton, 1991). K cells differed from this pattern only in the

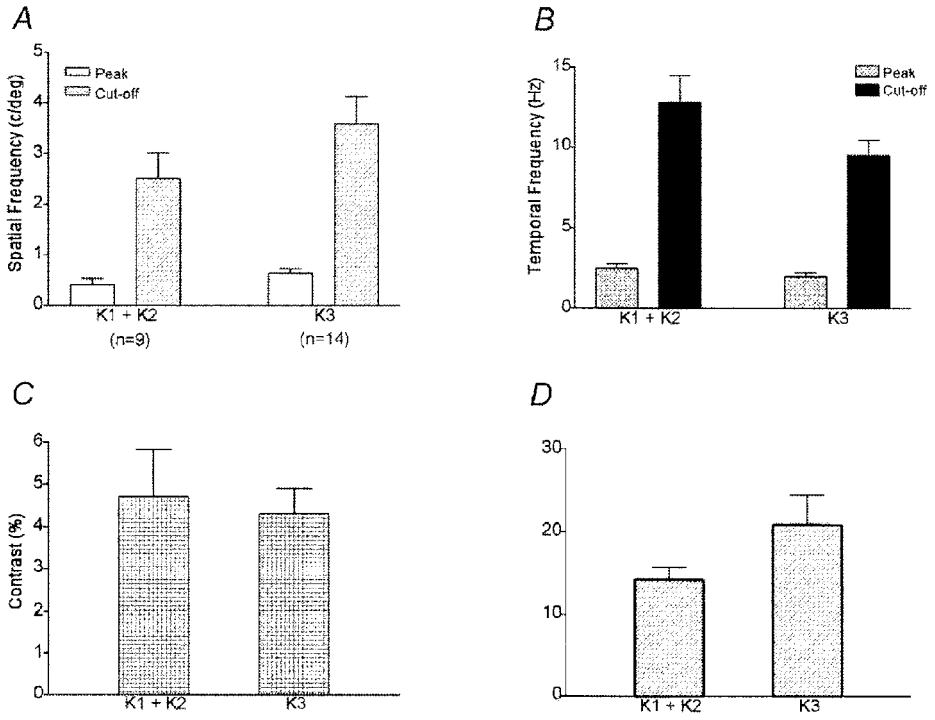

Figure 10. Spatial and temporal characteristics and contrast sensitivity of K cells in different layers

A, the mean peak SF was 0·42 ± 0·12 cycles deg^{-1} for K1/K2 cells ($n = 9$) and 0·64 ± 0·10 cycles deg^{-1} for K3 cells ($n = 14$). The mean SF cut-off was 2·5 ± 0·5 cycles deg^{-1} for K1/K2 cells and 3·6 ± 0·5 cycles deg^{-1} for K3. Peak SF and SF cut-off did not differ significantly between K1/K2 and K3 cells. *B*, the average peak TF was 2·44 ± 0·29 Hz for K1/K2 cells and 1·96 ± 0·23 Hz for K3 cells. The average TF cut-off was 12·8 ± 1·7 Hz for K1/K2 cells and 9·5 ± 0·9 Hz for K3 cells. Peak TF did not differ significantly between K1/K2 cells and K3 cells, but K1/K2 cells had a significantly higher TF cut-off than K3 cells (Mann-Whitney *U* test; $P \leqslant 0{\cdot}05$). *C*, the mean contrast threshold was 4·7 ± 1·1 for K1/K2 cells and 4·3 ± 0·6 for K3 cells, values not significantly different. *D*, the mean contrast gain was 14·2 ± 1·5 for K1/K2 cells and 20·9 ± 3·6 for K3 cells. Contrast gain did not differ significantly between K1/K2 cells and K3 cells.

overall degree of variation in centre size. Some K cells had significantly larger receptive field centre sizes than P or M cells at the same eccentricities, but other K cells had receptive field centre sizes that fell in the range of the smallest we encountered. K cells in bush babies and marmosets have relatively larger receptive field centres than those of P and M cells at the same eccentricities and the variability in K cell size is also higher than that of P and M cells (Norton & Casagrande, 1982; Irvin *et al.* 1993; A. J. White, S. G. Solomon & P. R. Martin, unpublished observations). In marmosets, however, M cells also show high variability in size (A. J. White, S. G. Solomon & P. R. Martin, unpublished observations). Receptive field centre sizes for P cells are smaller than those of M cells at any eccentricity (Sherman *et al.* 1976; Norton & Casagrande, 1982; Derrington & Lennie, 1984; Irvin *et al.* 1993; O'Keefe *et al.* 1998; Usrey & Reid, 2000). In owl monkeys two reports (O'Keefe *et al.* 1998; Usrey & Reid, 2000) have shown that receptive field sizes of P cells are smaller than those of M cells at all eccentricities. P and M cell receptive fields in owl monkeys were also found to be larger than those of macaque monkeys by a factor of about 2 and smaller than those of the bush baby by a factor of 2 which fits with the differences in visual acuity of these three primate species (O'Keefe *et al.* 1998). Although our data are generally consistent with these results, we find more overlap between the P and M receptive field sizes than was reported previously in owl monkeys. Notably, although P cells in macaque monkeys have been found to have smaller centres than M cells at matched eccentricities, significant overlap also has been reported (Derrington & Lennie, 1984; Spear *et al.* 1994; see Merigan & Maunsell, 1993 for review).

Spatial summation

Linearity of spatial summation is useful in distinguishing cell classes in cat LGN, but its usefulness in primate LGN cell classification remains controversial (see Casagrande & Norton, 1991 for review). We found that all K, P and M cells, with the exception of one M cell, were linear. Because we examined spatial linearity at the highest spatial frequency to which each cell would respond, we believe it is unlikely that we failed to drive non-linear subunits adequately and so missed a population of non-linear LGN cells. Consistent with our results, Usrey & Reid (2000) report that all the M and P cells in owl monkey and squirrel monkey LGN (K cells were not examined) are linear as measured by a null test. Additionally, counterphase gratings revealed very few spatially non-linear LGN cells in bush babies that resemble Y cells in cats (Norton & Casagrande, 1982). In macaque monkeys and marmosets, however, variable percentages of non-linear LGN cells have been reported (Kaplan & Shapley, 1982; Marrocco *et al.* 1982; Derrington & Lennie, 1984; Blakemore & Vital-Durand, 1986; A. J. White, S. G. Solomon & P. R. Martin, unpublished observations). In macaque monkeys, for example, the reported numbers of non-linear M cells have ranged from a high of 63% (Marrocco *et al.* 1982) to a low of 5·7% (Derrington & Lennie, 1984). In a recent study in marmosets, 11% of M cells, 6% of P cells and 13% of K cells were found to be spatially non-linear (A. J. White, S. G. Solomon & P. R. Martin, unpublished observations). Regardless, it appears that non-linearity of spatial summation is not a consistent feature of LGN cells in primates. At present it is unclear why some species have some spatially non-linear LGN cells while others have virtually none.

Spatial and temporal resolution

Although statistically demonstrable differences can be found in the spatial and temporal resolutions of owl monkey K, P and M cells, there is substantial overlap between the populations. Cells in all three classes could therefore contribute jointly to different aspects of conventional visual processing depending upon the demands of the task. At matched eccentricities, however, K cells exhibited lower spatial frequency cut-offs on average than did P and M cells. Furthermore, K cells showed temporal resolution values intermediate to those of the P and M cells. The contrast thresholds and contrast gains of K cells were more similar to those of M cells than those of P cells.

We found that M cells tended to exhibit lower spatial resolution and higher temporal resolution and contrast gain values than P cells. This is consistent with previous reports from owl monkeys and other simian and prosimian primates (Kaplan & Shapley, 1982; Hicks *et al.* 1983; Derrington & Lennie, 1984; Blakemore & Vital-Durand, 1986; Norton *et al.* 1988; O'Keefe *et al.* 1998; Usrey & Reid, 2000; A. J. White, S. G. Solomon & P. R. Martin, unpublished observations). O'Keefe *et al.* (1998) report that P cells in owl monkey LGN have higher spatial frequency cut-offs, lower optimal temporal frequencies and cut-offs and lower levels of responsivity than M cells. Our results are consistent with these findings, except that our data suggest that the P and M cells preferred similar peak temporal frequencies. Both our work and that of O'Keefe *et al.* (1998) found that the differences between owl monkey M and P cells in contrast sensitivity and gain are markedly lower than those reported for macaque M and P cells (Kaplan & Shapley, 1982; Hicks *et al.* 1983; Derrington & Lennie, 1984; Spear *et al.* 1994).

Physiological subclasses of K cells

In owl monkeys the different K layers (K1/K2 *vs.* K3) have distinct axonal termination patterns in V1. Axons from K3 cells mainly terminate within the cytochrome oxidase (CO) blobs in layer III of V1 and axons from cells in K1/K2 mainly terminate in cortical layer I (Ding & Casagrande, 1997). These anatomical differences suggest that some physiological differences may exist between these populations. Indeed, our results show that K cells in K1/K2 are more selective for lower spatial frequencies and higher temporal frequencies than cells in layer K3. Thus the K cells (K1/K2) that lie between or below the M layers tend to resemble M cells in resolution whereas the K3 cells have resolution values that lie between the average values for M and P cells (at least in terms of temporal resolution)

matching their anatomical position between the LGN M and P layers.

The distribution of the peak spatial frequencies of K cells also exhibits two modes, thus suggesting subclasses. Interestingly, M cells also showed double peaks within their distributions of spatial and temporal frequency cut-offs indicating the existence of M subclasses. The presence of M subclasses is consistent with anatomical work in owl monkeys (Boyd *et al.* 2000) and anatomical and modelling data in macaque monkeys (Lund *et al.* 1995; Bauer *et al.* 1999).

Additional support for the existence of K subclasses comes from the preliminary immunocytochemical work (Song *et al.* 2000) which shows that K cells in macaque monkeys are neurochemically diverse. Two marker proteins used to identify K cells in macaque monkeys, calbindin-D28k and the alpha form of calcium–calmodulin-dependent kinase II (αCaMK II), do not completely overlap in their distributions within the different LGN K layers. In fact, three subclasses of K cells could be identified by double-label immunocytochemistry. One subclass contained calbindin-D28k only, the second subclass contained αCaMK II only, and the third contained both proteins. The proportion of each type was found to vary within the different K layers suggesting that even within K layers different subclasses of K cells may co-exist.

A role for K cells in vision

Our physiological results from owl monkeys cannot directly address the most interesting question; namely, what role do K cells play in the vision of primates? These data, however, do provide descriptions of K cell response characteristics from which we can draw a few conclusions. The first is that K cells in owl monkeys are a heterogeneous population. The idea that K cells contain subclasses is supported both by work in the nocturnal prosimian bush baby (Irvin *et al.* 1986) and work in the diurnal simian marmoset (Martin *et al.* 1997; White *et al.* 1998; Solomon *et al.* 1999; A. J. White, S. G. Solomon & P. R. Martin, unpublished observations). K cells in marmosets are heterogeneous with some responding to colour (blue-ON), others responding only to achromatic gratings and still others being unresponsive to gratings.

Our physiological results in owl monkey and comparable data in bush babies suggest that many K cells exhibit spatial and temporal resolution values in the range that would allow these cells to contribute to conventional aspects of spatial and temporal vision. If this is true, why is the anatomy of the K pathway so different from that of the P and M pathways? Why do K cells send their axons either to cortical layer I or to the CO blobs within cortical layer III and not to a subdivision of layer IV as is the case with M and P LGN cells? Casagrande (1994) suggested that clues about the K pathway might be gained by examining the role of the target cells (CO blobs) of the K pathway as well as any extraretinal inputs that are unique to K cells. What comes to mind first about the CO blobs is colour vision, based upon the famous papers by Livingstone & Hubel (1984, 1988). They suggested that cells in the CO blobs are tuned specifically to chromatic stimuli. The finding of blue-ON K cells in marmosets fits with this hypothesis, but is inconsistent with the fact that CO blobs are ubiquitously well developed in all primates and that K cells project to CO blobs in all primates examined, but blue cones are absent in the nocturnal owl monkey and in the bush baby (Wikler & Rakic, 1990; Jacobs *et al.* 1993). Clearly K cells, CO blobs, and the anatomy of this pathway are highly conserved features across primates. Perhaps some K cells contribute uniquely to brightness contrast information but also colour contrast in species that have colour vision. Alternatively, K cells could contribute to a variety of other aspects of vision that might be tested adequately only in the awake behaving preparation. The subgroup of K cells that do not respond well to gratings could, for example, contribute to eye movement-related signals because K LGN cells in all primates receive a direct input from the superficial layers of the superior colliculus (input that P and M cells lack), and because a significant number of K cells project indirectly to the dorsal medial visual area (DM), an area concerned more with motion than with object vision (Harting *et al.* 1980, 1991; Beck & Kaas, 1998, 1999).

Finally, the neurochemistry and projection patterns of some K cells indicate that they are part of a neuromodulatory pathway. LGN K cells and cells within the adjacent inferior pulvinar nucleus are similar in that they both contain calbindin (Jones & Hendry, 1989). Both K cells and the inferior pulvinar cells project to layer I, the most superficial layer of V1 (Ogren & Hendrickson, 1977; Carey *et al.* 1979). Projections to layer I in all cortical regions are in a position to modulate signals within all cortical layers because the apical dendrites of the majority of cortical neurons extend into layer I (Vogt, 1991). Moreover, some investigators have proposed that the pulvinar nucleus is involved in visual attention (see Robinson & Petersen, 1992 for review). Perhaps some of the K cells that respond poorly in the anaesthetized animal project to layer I and are active along with the pulvinar cells in regulating visual attention. Future work in which K cells can be queried with an electrode in awake behaving monkeys may be able to more directly address these hypotheses.

Albrecht, D. G. & Hamilton, D. B. (1982). Striate cortex of monkey and cat: Contrast response function. *Journal of Neurophysiology* **48**, 217–237.

Barlow, H. B. & Levick, W. R. (1969). Changes in the maintained discharge with adaptation level in the cat retina. *Journal of Physiology* **202**, 699–778.

Bauer, U., Scholz, M., Levitt, J. B., Obermayer, K. & Lund, J. S. (1999). A model for the depth-dependence of receptive field size and contrast sensitivity of cells in layer 4C of macaque striate cortex. *Vision Research* **39**, 613–629.

Beck, P. D. & Kaas, J. H. (1998). Cortical connections of the dorsomedial visual area in New World owl monkeys (*Aotus trivirgatus*) and squirrel monkeys (*Saimiri sciureus*). *Journal of Comparative Neurology* **400**, 18–34.

Beck, P. D. & Kaas, J. H. (1999). Cortical connections of the dorsomedial visual area in Old World macaque monkeys. *Journal of Comparative Neurology* **406**, 487–502.

Blakemore, C. & Vital-Durand, F. (1986). Organization and post-natal development of the monkey's lateral geniculate nucleus. *Journal of Physiology* **380**, 453–491.

Boyd, J. D., Casagrande, V. A. & Bonds, A. B. (1998). How distinct are the lateral geniculate nucleus (LGN) inputs to areas 17 and 18 in the cat? *Society for Neuroscience Abstracts* **28**, 894.

Boyd, J. D. & Matsubara, J. A. (1996). Laminar and columnar patterns of geniculocortical projections in the cat: Relationship to cytochrome oxidase. *Journal of Comparative Neurology* **365**, 659–682.

Boyd, J. D., Mavity-Hudson, J. A. & Casagrande, V. A. (2000). The connections of layer 4 subdivisions in the primary visual cortex (V1) of the owl monkey. *Cerebral Cortex* **10**, 644–662.

Brodmann, K. (1909). *Localization in the Cerebral Cortex*, translated and edited by L. J. Garey from *Vergleichen lokalisationslehre der grosshirnrinde in ihren prinzipien dargestellt auf grund des zellenbaues* (Johann Ambrosius Barth, Leipzig), pp. 37–59. Smith-Gordon and Co. Ltd, London.

Carey, R. G., Fitzpatrick, D. & Diamond, I. T. (1979). Layer I of striate cortex of *Tupaia glis* and *Galago senegalensis*: Projections from thalamus and claustrum revealed by retrograde transport of horseradish peroxidase. *Journal of Comparative Neurology* **186**, 393–437.

Casagrande, V. A. (1994). A third parallel visual pathway to primate area V1. *Trends in Neurosciences* **17**, 305–310.

Casagrande, V. A. (1999). The mystery of the visual system K pathway. *Journal of Physiology* **517**, 630.

Casagrande, V. A. & Kaas, J. H. (1994). The afferent, intrinsic, and efferent connections of primary visual cortex. In *Cerebral Cortex*, vol. 10, *Primary Visual Cortex of Primates*, ed. Peters, A. & Rockland, K. S., pp. 201–259. Plenum Press, New York.

Casagrande, V. A. & Norton, T. T. (1991). The lateral geniculate nucleus: A review of its physiology and function. In *The Neural Basis of Visual Function*, ed. Leventhal, A. G., vol. 4, *Vision and Visual Dysfunction* series, ed. Cronley-Dillon, J. R., pp. 41–84. MacMillan Press, London.

Chapman, B., Zahs, K. R. & Stryker, M. P. (1991). Relation of cortical cell orientation selectivity to alignment of receptive fields of the geniculocortical afferents that arborize within a single orientation column in ferret visual cortex. *Journal of Neuroscience* **11**, 1347–1358.

DeBruyn, E. J., Casagrande, V. A., Beck, P. D. & Bonds, A. B. (1993). Visual resolution and sensitivity of single cells in the primary visual cortex (V1) of a nocturnal primate (bush baby): Correlations with cortical layers and cytochrome oxidase patterns. *Journal of Neurophysiology* **69**, 3–18.

Derrington, A. M. & Lennie, P. (1984). Spatial and temporal contrast sensitivities of neurons in lateral geniculate nucleus of macaque. *Journal of Physiology* **357**, 219–240.

DeYoe, E. A. & Van Essen, D. C. (1988). Concurrent processing streams in monkey visual cortex. *Trends in Neurosciences* **11**, 219–226.

Ding, Y. & Casagrande, V. A. (1997). The distribution and morphology of LGN K pathway axons within the layers and CO blobs of owl monkey V1. *Visual Neuroscience* **14**, 691–704.

Edwards, D. P., Purpura, K. P. & Kaplan, E. (1995). Contrast sensitivity and spatial frequency response of primate cortical neurons in and around the cytochrome oxidase blobs. *Vision Research* **35**, 1501–1523.

Enroth-Cugell, C. & Robson, J. (1966). The contrast sensitivity of retinal ganglion cells of the cat. *Journal of Physiology* **187**, 517–552.

Goodchild, A. K. & Martin, P. R. (1998). The distribution of calcium-binding proteins in the lateral geniculate nucleus and visual cortex of a New World monkey, the marmoset, *Callithrix jacchus*. *Visual Neuroscience* **15**, 625–642.

Harting, J. K., Huerta, M. F., Frankfurter, A. J., Strominger, N. L. & Royce, G. J. (1980). Ascending pathways from the monkey superior colliculus: An autoradiographic analysis. *Journal of Comparative Neurology* **192**, 853–882.

Harting, J. K., Huerta, M. F., Hashikawa, T. & Van Lieshout, D. P. (1991). Projection of the mammalian superior colliculus upon the dorsal lateral geniculate nucleus: Organization of tectogeniculate pathways in nineteen species. *Journal of Comparative Neurology* **304**, 275–306.

Hendry, S. H. & Yoshioka, T. (1994). A neurochemically distinct third channel in the macaque dorsal lateral geniculate nucleus. *Science* **264**, 575–577.

Hendry, S. H. & Reid, R. C. (2000). The koniocellular pathway in primate vision. *Annual Review of Neuroscience* **23**, 127–153.

Henry, G. H., Bishop, P. O., Tupper, R. M. & Dreher, B. (1973). Orientation specificity and response variability of cells in the striate cortex. *Vision Research* **13**, 1771–1779.

Hicks, T. P., Lee, B. B. & Vidyasagar, T. R. (1983). The responses of cells in macaque lateral geniculate nucleus to sinusoidal gratings. *Journal of Physiology* **337**, 183–200.

Hochstein, S. & Shapely, R. M. (1976). Quantitative analysis of retinal ganglion cell classifications. *Journal of Physiology* **262**, 237–264.

Hubel, D. H. & Livingstone, M. S. (1990). Color and contrast sensitivity in the lateral geniculate body and primary visual cortex of the macaque monkey. *Journal of Neuroscience* **10**, 2223–2237.

Irvin, G. E., Casagrande, V. A. & Norton, T. T. (1993). Center/surround relationships of magnocellular, parvocellular, and koniocellular relay cells in primate lateral geniculate nucleus. *Visual Neuroscience* **10**, 363–373.

Irvin, G. E., Norton, T. T., Sesma, M. A. & Casagrande, V. A. (1986). W-like response properties of interlaminar zone cells in the lateral geniculate nucleus of a primate (*Galago crassicaudatus*). *Brain Research* **362**, 254–270.

Jacobs, G. H., Deegan, J. F., Neitz, J., Crognale, M. A. & Neitz, M. (1993). Photopigments and color vision in the nocturnal monkey, *Aotus*. *Vision Research* **33**, 773–783.

Jacobs, G. H., Neitz, M. & Neitz, J. (1996). Mutations in S-cone pigment genes and the absence of colour vision in two species of nocturnal primate. *Proceedings of the Royal Society* B **263**, 705–710.

Johnson, J. K. & Casagrande, V. A. (1995). The distribution of calcium-binding proteins within the parallel visual pathways of a primate (*Galago crassicaudatus*). *Journal of Comparative Neurology* **356**, 238–260.

Jones, E. G. & Hendry, S. H. C. (1989). Differential calcium binding protein immunoreactivity distinguishes classes of relay neurons in monkey thalamic nuclei of primates. *Journal of Comparative Neurology* **182**, 517–554.

Kaplan, E. & Shapley, R. M. (1982). X and Y cells in the lateral geniculate nucleus of macaque monkeys. *Journal of Physiology* **330**, 125–143.

Kremers, J., Weiss, S. & Zrenner, E. (1997). Temporal properties of marmoset lateral geniculate cells. *Vision Research* **37**, 2649–2660.

Lachica, E. A., Beck, P. D. & Casagrande, V. A. (1992). Parallel pathways in macaque monkey striate cortex: Anatomically defined columns in layer III. *Proceedings of the National Academy of Sciences of the USA* **89**, 3566–3570.

Lachica, E. A. & Casagrande, V. A. (1992). Direct W-like geniculate projections to the cytochrome oxidase (CO) blobs in primate visual cortex: Axon morphology. *Journal of Comparative Neurology* **319**, 141–158.

Lennie, P., Krauskopf, J. & Sclar, G. (1990). Chromatic mechanisms in striate cortex of macaque. *Journal of Neuroscience* **10**, 649–669.

Leventhal, A. G., Thompson, K. G., Liu, D., Zhou, Y. & Ault, S. J. (1995). Concomitant sensitivity to orientation, direction, and color of cells in layers 2, 3, and 4 of monkey striate cortex. *Journal of Neuroscience* **15**, 1808–1818.

Livingstone, M. S. & Hubel, D. H. (1984). Anatomy and physiology of a color system in the primate visual cortex. *Journal of Neuroscience* **4**, 309–356.

Livingstone, M. S. & Hubel, D. H. (1988). Segregation of form, color, movement and depth: Anatomy, physiology, and perception. *Science* **240**, 740–749.

Lund, J., Wu, Q., Hadingham, P. T. & Levitt, J. B. (1995). Cells and circuits contributing to functional properties in area V1 of macaque monkey cerebral cortex: Bases for neuroanatomically realistic models. *Journal of Anatomy* **187**, 563–581.

Marrocco, R. T., McClurkin, J. W. & Young, R. A. (1982). Spatial summation and conduction latency classification of cells of the lateral geniculate nucleus of macaques. *Journal of Neuroscience* **2**, 1275–1291.

Martin, P. R., White, A. J. R., Goodchild, A. K., Wilder, H. D. & Sefton, A. E. (1997). Evidence that blue-on cells are part of the third geniculocortical pathway in primates. *European Journal of Neuroscience* **9**, 1536–1541.

Merigan, W. H. & Maunsell, J. H. R. (1993). How parallel are the primate visual pathways? *Annual Review of Neuroscience* **16**, 369–402.

Norton, T. T. & Casagrande, V. A. (1982). Laminar organization of receptive-field properties in lateral geniculate nucleus of bush baby (*Galago crassicaudatus*). *Journal of Neurophysiology* **47**, 715–741.

Norton, T. T., Casagrande, V. A., Irvin, G. E., Sesma, M. A. & Petry, H. M. (1988). Contrast-sensitivity functions of W-, X-, and Y-like relay cells in the lateral geniculate nucleus of bush baby, *Galago crassicaudatus*. *Journal of Neurophysiology* **59**, 1639–1656.

Ogren, M. P. & Hendrickson, A. E. (1977). The distribution of pulvinar terminals in visual areas 17 and 18 of the monkey. *Brain Research* **137**, 343–350.

O'Keefe, L. P., Levitt, J. B., Kipper, D. C., Shapley, R. M. & Movshon, J. A. (1998). Functional organization of owl monkey lateral geniculate nucleus and visual cortex. *Journal of Neurophysiology* **80**, 594–609.

Reid, R. C. & Shapley, R. M. (1992). Spatial structure of cone inputs to receptive fields in primate lateral geniculate nucleus. *Nature* **356**, 716–718.

Robinson, D. L. & Petersen, S. E. (1992). The pulvinar and visual salience. *Trends in Neurosciences* **15**, 127–132.

Sherman, S. M., Wilson, J. R., Kaas, J. H. & Webb, S. V. (1976). X- and Y-cells in the dorsal lateral geniculate nucleus of the owl monkey (*Aotus trivirgatus*). *Science* **192**, 475–477.

Solomon, S. G., White, A. R & Martin, P. R. (1999). Temporal contrast sensitivity in the lateral geniculate nucleus of a New World monkey, the marmoset *Callithrix jacchus*. *Journal of Physiology* **517**, 907–917.

Song, Z., Mavity-Hudson, J. & Casagrande, V. A. (2000). Diversity of neurochemical properties of koniocellular cells in the lateral geniculate nucleus (LGN) of macaque monkeys. *Society for Neuroscience Abstracts* **30**, 1198.

Spear, P. D., Moore, R. J., Kim, C. B. Y., Xue, J.-T. & Tumosa, N. (1994). Effects of aging on the primate visual system: Spatial and temporal processing by lateral geniculate neurons in young adult and old rhesus monkeys. *Journal of Neurophysiology* **72**, 402–420.

Sur, M. & Sherman, S. M. (1982). Linear and non-linear W cells in C laminae of the cat's lateral geniculate nucleus. *Journal of Neurophysiology* **47**, 869–884.

Usrey, W. M. & Reid, R. C. (2000). Visual physiology of the lateral geniculate nucleus in two species of New World monkey: *Saimiri sciureus* and *Aotus trivirgatis*. *Journal of Physiology* **523**, 755–769.

Vogt, B. A. (1991). The role of layer I in cortical function. In *Cerebral Cortex*, vol. 9, *Normal and Altered States of Functions*, ed. Peters, A. & Jones, E. G. pp. 49–80. Plenum Press, New York.

White, A. J., Wilder, H. D., Goodchild, A. K., Sefton, A. J. & Martin, P. R. (1998). Segregation of receptive field properties in the lateral geniculate nucleus of a New World monkey, the marmoset *Callithrix jacchus*. *Journal of Neurophysiology* **80**, 2063–2076.

Wikler, K. C. & Rakic, P. (1990). Distribution of photoreceptor subtypes in the retina of diurnal and nocturnal primates. *Journal of Neuroscience* **10**, 3390–3401.

Xu, X. M., Boyd, J., Allison, J. D., Ichida, J., Bonds, A. B. & Casagrande, V. (1999). Receptive field properties of K cells in the lateral geniculate nucleus (LGN) of owl monkeys (*Aotus trivirgatus*). *Society for Neuroscience Abstracts* **29**, 1427.

Zar, J. H. (1999). *Biostatistical Analysis*, 4th edn, pp. 195–199. Prentice-Hall, Inc., New Jersey.

Acknowledgements

We would like to thank Andrew Tomarken, Jeffrey Schall, Amy Wiencken, Gyula Sáry, Yuri Shostak and David Royal for helpful comments on the manuscript. We would also like to thank Julie Mavity-Hudson for excellent technical assistance. This work was supported by grants EY01778 (V.A.C.), EY03778 (A.B.B.) and core grants EY08126 and HD 15052.

Corresponding author

V. A. Casagrande: Department of Cell Biology, Vanderbilt Medical School, Medical Center North C2310, Nashville, TN 37232-2175, USA.

Email: vivien.casagrande@mcmail.vanderbilt.edu

Author's present address

J. D. Boyd: Department of Biological Sciences, Simon Fraser University, 8888 University Drive, Burnaby, British Columbia, Canada V5A 1S6.